Development 129, 2087-2098 (2002)
Printed in Great Britain © The Company of Biologists Limited 2002
DEV1774

A mitogen gradient of dorsal midline Wnts organizes growth in the CNS

Sean G. Megason and Andrew P. McMahon

Department of Molecular and Cellular Biology, Harvard University, Cambridge, MA 02138, USA
e-mail: amcmahon@mcb.harvard.edu or megason@hombiosys.com

Accepted 8 February 2002

SUMMARY

Cell cycle progression and exit must be precisely patterned during development to generate tissues of the correct size, shape and symmetry. Here we present evidence that dorsal-ventral growth of the developing spinal cord is regulated by a Wnt mitogen gradient. Wnt signaling through the β-catenin/TCF pathway positively regulates cell cycle progression and negatively regulates cell cycle exit of spinal neural precursors in part through transcriptional regulation of *cyclin D1* and *cyclin D2*. Wnts expressed at the dorsal midline of the spinal cord, Wnt1 and Wnt3a, have mitogenic activity while more broadly expressed Wnts do not. We present several lines of evidence suggesting that dorsal midline Wnts form a dorsal to ventral concentration gradient. A growth gradient that correlates with the predicted gradient of mitogenic Wnts emerges as the neural tube grows with the proliferation rate highest dorsally and the differentiation rate highest ventrally. These data are rationalized in a 'mitogen gradient model' that explains how proliferation and differentiation can be patterned across a growing field of cells. Computer modeling demonstrates this model is a robust and self-regulating mechanism for patterning cell cycle regulation in a growing tissue.

Supplemental data available on-line

Key words: Spinal cord, Wnts, Growth gradient, Cell cycle gradient, Chick

INTRODUCTION

Embryonic development is the execution of a program encoded in an organism's genome. In the past decade, we have elucidated a great deal about the individual lines of code in this developmental program but much less about how these lines of code integrate at a systems level to generate a properly patterned and proportioned organism. A salient example of the gap in our knowledge is growth regulation. Embryonic growth is determined at the cellular level by the rates and patterns of cell growth, cell division, cell cycle exit and cell death. The molecular mechanisms that regulate these different cellular behaviors are well understood (Nurse, 2000), but little is known about how these cellular behaviors are coordinated in a developmental or evolutionary context to generate tissues and organisms of the proper size (Conlon and Raff, 1999; Day and Lawrence, 2000).

The spinal cord is an ideal model for studying the developmental regulation of growth. Firstly, mitotically active and post-mitotic cell populations in the spinal cord are spatially distinct. With the exception of the dorsomedial roof plate and the ventromedial floor plate, the medially located ventricular zone is an epithelium composed entirely of mitotically active, multipotent neural precursors. When neural precursors exit the cell cycle, they migrate laterally from the ventricular zone to the mantle zone, which is composed entirely of post-mitotic, differentiating neurons and glia. Secondly, the spinal cord's anatomy is simple and very well conserved between mice and chick allowing each of these experimental systems to be exploited and compared. Dorsally there are three classes of interneurons, D1, D2 and D3, that are involved in sensory processing. The ventral spinal cord contains motor neurons and four classes of interneurons, V0 through V3, that together are involved in regulating motor control (Tanabe and Jessell, 1996). Lastly, the mechanisms that specify cell fate in the spinal cord are well understood and well conserved between mice and chick (Lee and Jessell, 1999; Briscoe et al., 2000; Jessell, 2000). However, growth regulation in the spinal cord, that is, the mechanisms that pattern the rates of cell cycle progression and cell cycle exit of neural precursors to generate a spinal cord of the proper size and shape, are less well understood.

Wnts are a large family of secreted signaling proteins related to *Drosophila* Wingless (reviewed by Nusse, 2001). Several lines of evidence have implicated Wnts in the regulation of growth in the developing central nervous system. The midbrain is deleted in mice mutant for *Wnt1* (McMahon and Bradley, 1990; Thomas and Cappechi, 1990) and the hippocampus is deleted in *Wnt3a* mutants (Lee et al., 2000b). *Wnt1/Wnt3a* double mutant mice have an additional reduction of the caudal diencephalon, rostral hindbrain and cranial and spinal ganglia (Ikeya et al., 1997) (S. Lee, M. Ishibashi and A. P. M., unpublished) suggesting that Wnt1 and Wnt3a play broad, semi-redundant roles in growth control in the neural tube rather than simply specifying regional cell fates. Consistent with this view, ectopic expression of *Wnt1* in transgenic mice causes an overgrowth of the neural tube without altering the primary patterning of cell identities along the DV axis (Dickinson et al., 1994). Together the available data indicate that Wnts often regulate tissue growth rather than cell

fate but do not identify the mechanism at a cellular level. We have explored these mechanisms in the context of the developing vertebrate spinal cord.

MATERIALS AND METHODS

DNA cloning

pCIG (Fig. 1a) was made by linker insertion of three nuclear localization sequences into pIRES2-EGFP (Clontech) and transferring this insert to pCAGGS (Niwa et al., 1991). All constructs were trimmed of UTRs and given consensus translation initiation sequences. The following cDNA clones were inserted into pCIG: dominant active human β-catenin, dominant negative human TCF4 (Tetsu and McCormick, 1999), dominant negative cyclin D1 (Diehl and Sherr, 1997), and several mouse Wnts as indicated (Gavin et al., 1990) (A. P. M., unpublished). TOPRed and FOPRed were made by transferring the enhancer/promoter from TOPFLASH and FOPFLASH (Korinek et al., 1998) to pDsRed1-1 (Clontech).

Electroporation of spinal neural precursors

Quiagen purified, super-coiled plasmid DNA was injected into the neural tubes of Hamburger-Hamilton stage 10-11 chicken embryos at a concentration of 1.0 μg/μl in H_2O with 50 ng/μl Fast Green. For coinjections, pCIG was used at 200 ng/μl. Electrodes were made from 0.25 mm diameter platinum wire (Aldrich) and were 5 mm long and spaced 5 mm apart. Electrodes were placed flanking the neural tube, covered with a drop of PBS, and pulsed 3 times at 24 V for 50 mseconds with a BTX Electroporator (Genetronics).

Immunohistochemistry and in situ hybridization

Embryos were fixed overnight at 4°C in 4% paraformaldehyde in PBS with 0.1% Triton X-100, cryoprotected with 20% sucrose in PBS, and cryosectioned. For in situ hybridization on transfected embryos, GFP and ToPro3 (Molecular Probes) were visualized first. Frozen section in situ hybridization was performed using probes to mouse *Wnt1*, *Wnt3a*, *Wnt4*, *Wnt7a*, *Wnt7b* (Gavin et al., 1990), *Wnt3* (Roelink et al., 1990), *TCF3*, *TCF4* (Korinek et al., 1998), *cyclin D1* and *cyclin D2* (Matsushime et al., 1991) and chick *cyclin D1* (Lahti et al., 1997) and *cyclin D2* (Li et al., 1995). Antibodies to Pax6, Pax7, Nkx2.2, Isl1, MNR2, Lim2 and En1 were obtained from the Developmental Studies Hybridoma Bank developed under the auspices of the NICHD and maintained by The University of Iowa, Department of Biological Sciences, Iowa City, IA 52242.

Cell cycle analysis

For cumulative labeling, 150 μl of 5 μg/μl BrdU (bromodeoxyuridine) was applied on top of embryos in ovo. An additional 100 μl was applied every 4 hours. Frozen sections were first imaged for GFP and propidium iodide-stained DNA and then stained for neural specific β-tubulin III (clone TuJ1, Covance) and Alexa 488 (Molecular Probes) secondary. Sections were refixed in 4% paraformaldehyde for 30 minutes, incubated in 50% formamide, 1× SSC, 0.1% Tween at 65°C for 2 hours, rinsed, incubated in 2 M HCl for 15 minutes, 0.1 M $Na_2B_4O_7$ pH 8.5 for 10 minutes, rinsed, and stained using biotinylated anti-BrdU (Zymed), strepavidin-Cy5 (Jackson), and propidium iodide. The BrdU labeling index was taken as the percentage of BrdU-positive ventricular zone (N-tubulin negative) cells. The proliferation rate (mitoses/hour) is given by the slope of the regression line through the BrdU labeling indexes at 1, 2, 3, 4, 5, and 6 hours for at least 4 replicates. To calculate the differentiation rate (exits/hour) for a given stage, we first determined the change in the number of differentiated cells between stages by counting the number of N-tubulin-positive cells in sections. The change in the number of differentiated cells was then divided by the number of precursor cells to calculate the differentiative fraction. The differentiative fraction was divided by the developmental time difference between the two stages to get the differentiation rate.

RESULTS

Neural precursor cell cycle control by Wnts

Wnts could regulate tissue growth by controlling cell growth (an increase in the size of a cell), cell division, cell cycle exit, or cell death. We investigated the cellular mechanism through which Wnts regulate growth using in ovo electroporation (Nakamura et al., 2000) of the chick spinal cord. A construct named pCIG containing a CMV enhancer, β-actin promoter, and an internal ribosome entry sequence (IRES) followed by a nuclear localized green florescent protein (GFP) was developed to allow identification of transfected cells with single cell resolution (Fig. 1a). In ovo electroporation gave rapid (GFP expression was visible within 3 hours), unilateral, high-percentage transfection of spinal neural precursors (Fig. 1b,c).

To determine if Wnts act as mitogens for spinal neural precursors in the chick, we electroporated *pCIG-Wnt1* into the developing neural tube and measured its effects on the rates of proliferation and differentiation. We first assessed the level of transfection by visualizing GFP in cross sections of transfected neural tubes and then subjected the same sections to immunostaining for a post-mitotic neural marker, neural tubulin, and determined which cells were in S-phase of the cell cycle by examining incoporation of the thymidine analog BrdU. Ectopic expression of *Wnt1* reduced the number of differentiated neurons, as visualized by immunostaining for neural tubulin and increased the rate of neural precursor proliferation, as visualized by immunostaining for BrdU incorporation (Fig. 1d,e). The mitogenic effect of ectopic expression of *Wnt1* is especially pronounced at ventral levels where the ventricular zone on the transfected side often bulges ventrally beyond the control side (Fig. 1e). To quantify these DV differences, we determined the BrdU labeling index in 5 equally spaced bins across the DV axis in the transfected and non-transfected sides of the neural tube. Ectopic Wnt1 has no mitogenic effect on neural precursors in the dorsal one fifth of the ventricular zone, relative to the non-transfected side, but has a progressively greater effect on more ventral precursors (Fig. 1f). These data suggest that endogenous Wnt1 is saturating dorsally and progressively subsaturating ventrally.

To determine the rates of differentiation and proliferation in transfected embryos, we combined visualization of GFP to assess transfection with antibody staining for neural tubulin to monitor differentiation and the cumulative labeling method for cell cycle analysis using BrdU. Ectopic Wnt1 caused an approx. 50% increase in the proliferation rate of neural precursors in the ventral three fifths of the ventricular zone by increasing the fraction of cells in S-phase and thus shortening the lengths of G_1 and/or G_2 phases of the cell cycle (Fig. 1g). Ectopic Wnt1 reduced the differentiation rate of motor neurons and interneurons by 55% relative to the non-transfected side (Fig. 1h). The rates of apoptosis, as determined by TUNEL, and cell growth, as measured by cell size and density, were not affected (data not shown). These data show that Wnts can regulate tissue growth by controlling both cell cycle progression and cell cycle exit.

Wnt signals can be transduced through several pathways

(Kuhl et al., 2000). The 'canonical' pathway results in the stabilization of β-catenin that can then bind members of the TCF/Lef transcription factor family to activate transcription of Wnt targets. To see if mitogenic Wnt signaling in spinal neural precursors is transduced through the β-catenin pathway, we transfected dominant active and dominant negative constructs in this pathway. Transfection of a dominant active form of β-catenin that is resistant to targeted proteolysis resulted in an overgrowth phenotype similar to that induced by Wnt1 suggesting that the mitogenic action of Wnts in neural precursors is transduced through the β-catenin pathway (Fig. 2a). However, transfection of dominant active β-catenin causes a much more profound increase in neural precursor number and reduction in differentiation than does Wnt1 suggesting that one or more components in the transduction pathway between Wnt1 and β-catenin are rate limiting. Taken together with the different dorsal-ventral effects of ectopic Wnt1, these data suggest that normally a component of the transduction pathway between Wnt1 and β-catenin is rate-limiting at dorsal levels and as Wnt1 concentration decreases ventrally, Wnt ligand itself becomes rate limiting. Ectopic expression of dominant active β-catenin could bypass both of these rate-limiting steps to cause a more severe phenotype.

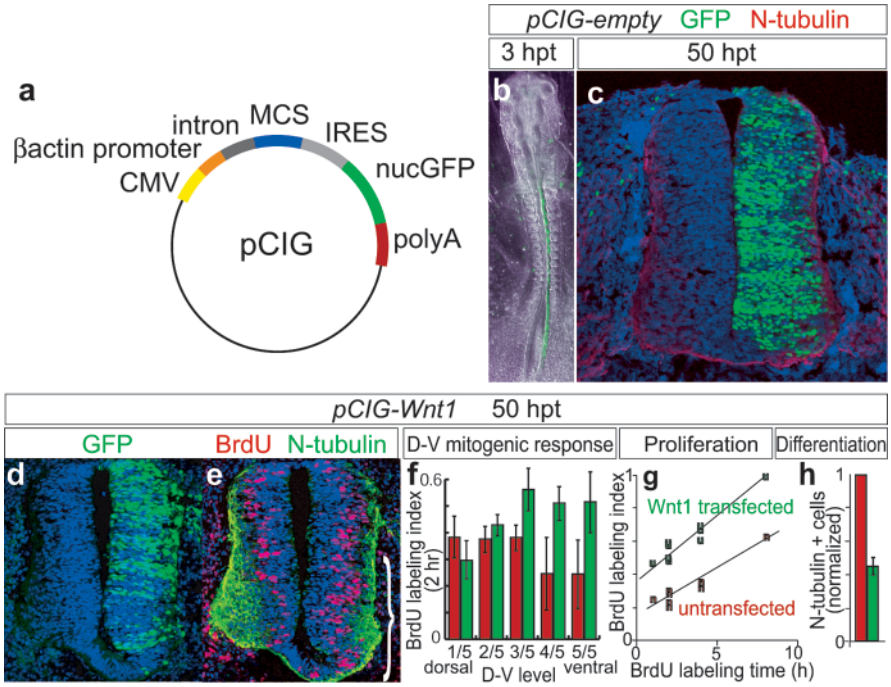

Fig. 1. Wnt1 promotes proliferation and inhibits differentiation. (a-c) Transfection of forelimb level chick spinal neural precursors by in ovo electroporation with a plasmid containing an internal ribosome entry sequence followed by nuclear GFP (a), gives rapid, ubiquitous, unilateral expression with cellular resolution and does not perturb normal development (b,c). (d,e) Embryos transfected with Wnt1 show an increase in BrdU incorporation (4 hour labeling) at ventral levels (marked by bracket) and a decrease in post-mitotic neurons marked with N-tubulin. (f-h) Rates of proliferation and differentiation were quantitated using BrdU cumulative labeling and N-tubulin staining in stage 22 embryos in both the transfected (green) and untransfected sides (red). Ectopic Wnt1 expression increased the BrdU labeling index to a progressively greater degree ventrally (f). BrdU cumulative labeling shows that ectopic Wnt1 increases both the proliferation rate and the fraction of cells in S-phase in the ventral three fifths of the ventricular zone (g). Wnt1 transfected precursors have a 55% reduction in the rate of differentiation (h).

We next performed marker analysis to determine if neural precursors across the DV axis are all responsive to Wnt/β-catenin signaling. Staining with cell type-specific antibodies shows that dominant active β-catenin reduced differentiation across the entire DV axis including D1, D2, D3 and V1 interneurons and motor neurons (Fig. 2b-d). Similar results were obtained on embryos transfected with *Wnt1* (data not shown). With longer periods of incubation after transfection (>52 hours post-transfection), dominant-active β-catenin induces apoptosis (data not shown). To show that the reduction in differentiation is not a secondary effect of increased apoptosis, we triple stained for GFP, TUNEL and Isl1 before there is much programmed cell death (34 hours post-transfection) to simultaneously visualize the transfection, apoptosis and differentiation of motor neurons. GFP-positive neural precursors are blocked from differentiating into motor neurons with no increase in the number of TUNEL-positive cells, showing that Wnt signaling can block differentiation of motor neurons prior to and independent of inducing apoptosis (Fig. 2e).

Wnt signaling could also affect proliferation and differentiation indirectly through altering the pattern of cell fate specification. To rule out this possibility, we examined the pattern of neural precursor cell types in embryos misexpressing dominant active β-catenin. Dominant active β-catenin caused an expansion of dorsal, intermediate, and ventral precursors as shown by staining for Pax7, Pax6, and Nkx2.2, but the order of these precursor domains and the boundaries between them is maintained (Fig. 2f-h). Ventral domains may be expanded relatively more than dorsal domains because, as shown below, the rate of proliferation is normally lower ventrally. These data show that Wnt signaling primarily regulates cell cycle progression and cell cycle exit rather than cell fate specification.

Studies in the mouse ventricular zone indicate that TCF3 and TCF4 are the predominant TCF/Lef family members that are expressed in spinal neural precursors (Cho and Dressler, 1998) (data not shown). To address whether TCF factors regulate the cell cycle, we expressed a dominant negative form of TCF4 that cannot interact with β-catenin and thus acts as a constitutive repressor of Wnt targets. Transfected cells as marked by GFP do not incorporate BrdU after 4 hours whereas incorporation was observed in neighboring non-transfected cells (arrows in Fig. 2i,j) showing that dominant negative TCF4 cell-autonomously blocks entry into S-phase of the cell cycle. Dominant negative TCF4-expressing cells, however, are not forced to differentiate and scattered GFP-positive cells can remain within the ventricular zone through stage 22 (data not shown). Together these data show that Wnt1 acting through

the β-catenin signaling pathway controls a developmental checkpoint in the cell cycle. Wnts can both promote G_1 to S progression to regulate proliferation and inhibit G_1 to G_0 cell cycle exit to regulate differentiation in precursor cells across the entire DV axis. These data also suggest that cell cycle withdrawal is necessary but not sufficient for neural differentiation at early stages of neural development.

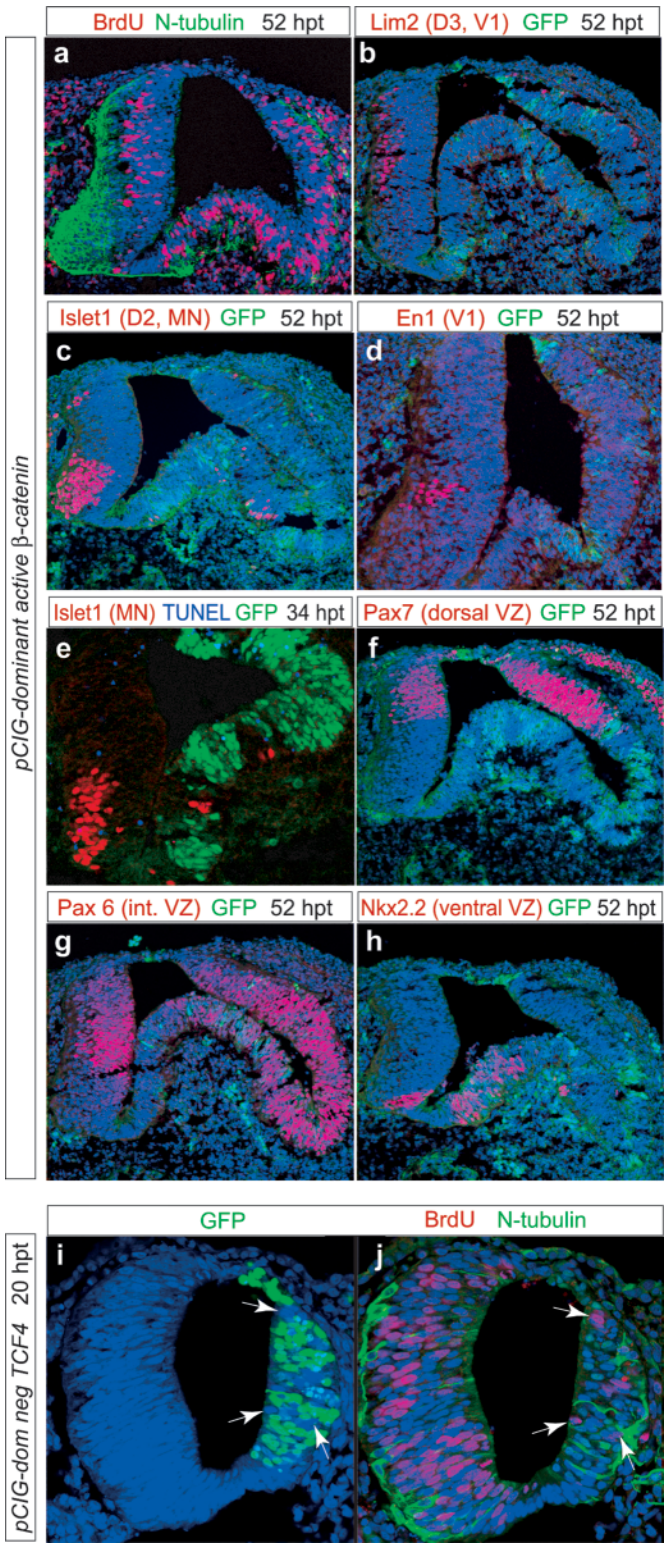

Mitogenic Wnt expression at the dorsal midline

We next investigated the relationship between where different Wnts are expressed in the spinal cord and their mitogenic activities to determine how their local activities might regulate the morphogenesis of the spinal cord. A number of Wnts are expressed in almost identical patterns in chick and mouse spinal cord (Parr et al., 1993; Hollyday et al., 1995). As only short sections of the chick cDNAs are available, we show their expression in the mouse and compare the activities of each mammalian Wnt-member in the chick model. As previously shown, *Wnt1* and *Wnt3a* are both expressed soon after the neural plate forms in the dorsal third of the neural tube. The expression of *Wnt1* and *Wnt3a* is restricted to the dorsal midline of the neural tube by E9.5, and remains only in the dorsal midline throughout morphogenesis of the spinal cord (Fig. 3a,c and not shown). *Wnt3* and *Wnt4* are also initially expressed in the dorsal third of the spinal cord, but as development proceeds their expression broadens ventrally to include the entire dorsal half of the ventricular zone (Fig. 3e,g). *Wnt7a* and *Wnt7b* are initially expressed at low levels throughout much of the ventricular zone and their expression increases at intermediate-ventral levels with time, until they are expressed at high levels throughout the ventral three quarters of the ventricular zone (Fig. 3i,k).

Interestingly, electroporation in the chick neural tube indicated that only *Wnt1* and *Wnt3a*, the two members whose expression is restricted to the dorsal midline, have mitogenic activity (Fig. 3a-l). *Wnt3*, *Wnt4*, *Wnt7a*, and *Wnt7b* had no effect on proliferation or differentiation of neural precursors relative to empty vector controls. Both *Wnt1* and *Wnt3a* caused an 80% increase in the BrdU labeling index in the ventral three fifths of the ventricular zone and a 50% reduction in differentiation (Fig. 3m,n). Wnt3, which is more similar to Wnt3a (84% amino acid identity) than Wnt3a is to Wnt1 (43% amino acid identity), surprisingly does not share the mitogenic activity or expression pattern of its close relative.

Regulation of G_1 cyclins by Wnts

We next investigated potential transcriptional targets of mitogenic Wnt signaling in neural precursors to address the mechanism through which they regulate the cell cycle and to determine the pattern of mitogenic Wnt response. Since, the activities of Wnt1 and Wnt3a suggest that they directly impinge on the cell cycle rather than regulate cell fate specification, we screened key components of the cell cycle

Fig. 2. Mitogenic Wnt signaling is transduced through the β-catenin/TCF pathway in neural precursors across the DV axis. (a) Dominant-active β-catenin causes a large expansion in the ventricular zone and a reduction in post-mitotic neurons. (b-d) Dominant-active β-catenin reduces D1, D2, D3, V1 and V2 interneurons and ventral motor neurons. (e) Triple staining for GFP, TUNEL and Isl1 shows that dominant-active β-catenin reduces differentiation of motorneurons prior to and independent of inducing apoptosis. (f-h) Dominant-active β-catenin causes precursor expansion at dorsal (f), intermediate (g), and ventral (h) levels without primarily changing positional information. (i,j) Dominant negative TCF4 cell-autonomously blocks precursors from entering S-phase of the cell cycle across the DV axis. Arrows mark cells on the transfected side that were not transfected (i) and are BrdU positive (j). All images are representative of at least 5 transfected embryos.

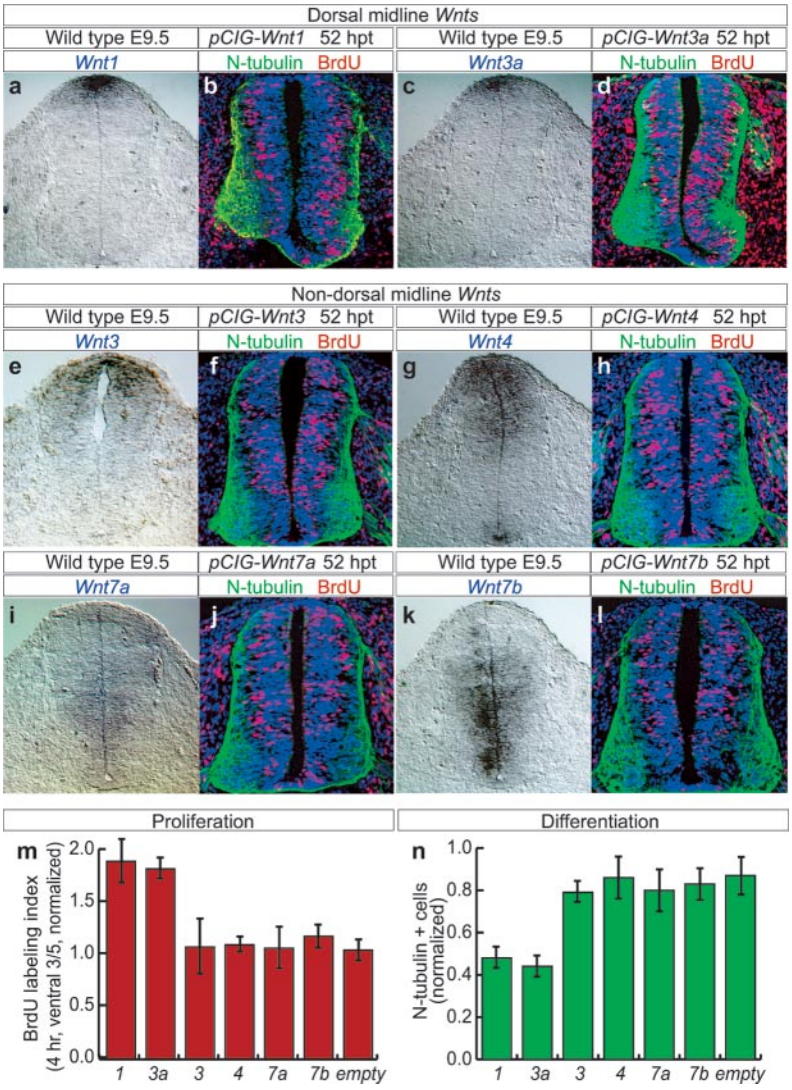

Fig. 3. Only dorsal midline Wnts have mitogenic activity. (a,c) *Wnt1* and *Wnt3a* have similar expression patterns in the dorsal midline. (b,d) Neural precursors transfected with *Wnt1* or *Wnt3a* have increased BrdU labeling index (4 hour incorporation) and a decreased number of post-mitotic neurons. (e,g) *Wnt3* and *Wnt4* are expressed in broad dorsal domains. *Wnt4* is also expressed in the floor plate (g). (i,k) *Wnt7a* and *Wnt7b* are expressed in broad ventral domains. (f,h,j,l) Neural precursors transfected with the non-dorsal midline Wnts, *Wnt3*, *Wnt4*, *Wnt7a* or *Wnt7b*, have normal BrdU incorporation and numbers of post-mitotic neurons. (m,n) The BrdU labeling index in the ventral three fifths of the VZ and the number of post-mitotic neurons were quantitated for these and other embryos. All sections were visualized for GFP to ensure good transfection before staining.

including cyclins, cyclin dependent kinases (CDKs), and CDK inhibitors (CKIs) as candidate targets. We found that *cyclin D1* is expressed throughout the early period of neural tube development in a dorsal to ventral gradient (highest dorsally) in mitotically active medial neural precursors in both mouse and chick (Fig. 4a-c, and data not shown). D-type cyclins are key regulators of G_1 exit. When the spinal cord is small, the gradient of cyclin D1 expression extends all the way across the ventricular zone but as the spinal cord grows the expression gradient becomes more dorsally restricted relative to the size of the DV axis (Fig. 4d).

To investigate the mechanism by which dorsal midline Wnts regulate the cell cycle of neural precursors, we examined the expression of cell cycle regulators in the neural tube of embryos transfected with Wnt signaling components. We found that transfection of dominant active *β-catenin* upregulates transcription of the G_1 cyclins *cyclin D1* and *cyclin D2* but not the G_2/M cyclins *cyclin A1* or *cyclin B3* in neural precursors (Fig. 4e-l). The locations of transfected cells were first determined by visualizing GFP and then the same sections were processed by in situ hybridization. Regions of the neural tube that ectopically express β-catenin have increased levels of *cyclin D1* and *cyclin D2* (Fig. 4e-h). Previous reports have found that β-catenin signaling upregulates *cyclin D1* but not *cyclin D2* in cultured cell lines and that the *cyclin D1* promoter contains consensus Lef/TCF binding sites required for this activity (Tetsu and McCormick, 1999; Shtutman et al., 1999). The transcriptional regulation of *cyclin D1* by Wnt signaling in neural precurors could thus be direct.

Ectopic expression of *Wnt1* or *Wnt3a* also upregulated *cyclin D1* expression (Fig. 4m,n and data not shown). However, in contrast to dominant active β-catenin, expression of *Wnt1* or *Wnt3a* only upregulated *cyclinD1* at intermediate to ventral levels. These data again suggest that endogenous mitogenic Wnts are saturating at dorsal levels (Fig. 4i,j and data not shown). As shown above, ventral precursors have a stronger mitogenic response to ectopic Wnt expression than do dorsal precursors. This dorsal-ventral pattern of mitogenic responsiveness of neural precursors to ectopic expression of *Wnt1* correlates with the pattern of *cyclin D1* upregulation (compare Fig. 4n and Fig. 1f). If activating Wnt signaling upregulates *cyclin D1* transcription, then attenuating Wnt signaling should downregulate *cyclin D1* transcription. Accordingly, high levels of expression of dominant negative TCF4 downregulated expression of *cyclin D1* (Fig. 4k,l).

To address how major a role transcriptional control of D-cyclins plays in the mitogenic response of Wnts, we ectopically expressed dominant negative and wild-type versions of cyclin D1. Transfection of a dominant negative cyclin D1 construct that forms abortive complexes with the G_1 cyclin dependent kinases CDK4 and CDK6 (Diehl and Sherr, 1997) reduced neural precursor expansion (Fig. 4q) but did not block neural cell cycle progression as severely as dominant negative TCF4. Ectopic expression of wild-type cyclin D1 was not sufficient to cause overgrowth of the neural tube as did Wnt1, Wnt3a, and dominant active β-catenin (data not shown). Additionally, mice mutant for *cyclin D1* have small eyes and reduced body size but are viable (Sicinski et al., 1995; Fantl et al., 1995). These data show that two key components of the cell cycle, *cyclin D1* and *cyclin D2*, are transcriptional targets of Wnt signaling in neural precursors but suggest other targets are also involved in the mitogenic response of neural precursors to Wnts.

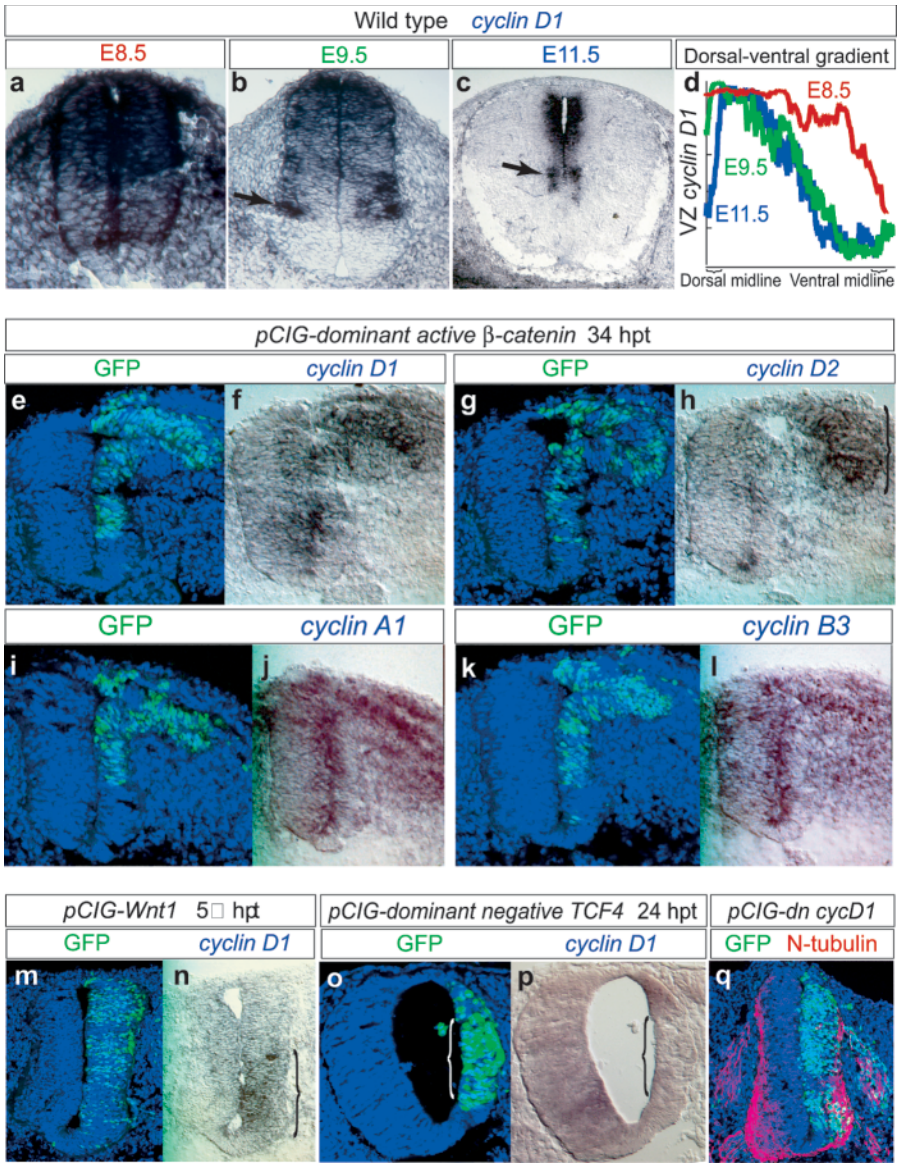

Fig. 4. Regulation of D-type cyclins by Wnts. (a-d) *cyclin D1* is expressed in a dorsal to ventral gradient. In situ hybridization at E8.5, E9.5 and E11.5 (a,b,c) shows *cyclin D1* is expressed in neural precursors in a DV gradient. *cyclin D1* is also transiently expressed in some differentiating neurons as marked by arrows in b and c. (d) Normalized quantitation of *cyclin D1* expression levels shows that the gradient extends completely across the DV axis when the spinal cord is small and becomes more dorsally restricted as the spinal cord grows. (e-q) Sections of transfected embryos were first visualized for GFP (e,g,i,k,m,o,q) and then stained by in situ hybridization (f,h,j,l,n,p). Dominant active β-catenin upregulates *cyclin D1* and *cyclin D2* (e-h). *cyclin D1* can be upregulated at all dorsal-ventral levels but *cyclin D2* can only be upregulated dorsally (upregulation marked by bracket). Dominant active β-catenin does not upregulate the expression of the G_2/M cyclins *cyclin A1* (i,j) or *cyclin B3* (k,l). Wnt1 upregulates *cyclin D1* expression at ventral levels but not at dorsal levels (upregulation marked by bracket) (m,n). Dominant negative TCF4 downregulates *cyclin D1* at all levels of high transfection efficiency as marked by bracket (o,p). Dominant negative *cyclin D1* reduces precursor expansion (q).

Converesely, it is likely that other regulatory elements in addition to the TCF binding sites contribute to the regulation of *cyclin D1* in the neural tube, especially its transient expression in apparently exiting cells. Taken together, these results support a model in which Wnt1 and Wnt3a expressed in the dorsal midline form a dorsal to ventral mitogen gradient that controls the graded expression of cell cycle regulators including D-type cyclins through the β-catenin pathway.

A dorsal-ventral gradient of Wnt signaling

High-affinity antibodies recognizing Wnt1 and Wnt3a are not available so we addressed the range of signaling of mitogenic Wnts by transfecting a transcriptional reporter for signaling through the β-catenin pathway into neural precursors. As our data suggests that mitogenic Wnt signals are transduced by the β-catenin pathway and only Wnts expressed in the dorsal midline appear to be mitogenic, this reporter might be expected to mark the range of activity of Wnts produced in the dorsal midline. Our reporter for Wnt/β-catenin signaling named pTOPRed contains synthetic Lef/TCF binding sites driving expression of red fluorescent protein. Coelectroporation of pTOPRed with pCIG was used to verify transfection by GFP expression (Fig. 5a). RFP from pTOPRed is expressed across the dorsal three quarters of the neural tube with highest expression in the dorsal quarter (Fig. 5b). By comparing the ratio of GFP expression to RFP expression, pTOPRed reveals a gradient of Wnt/β-catenin signaling across much of the DV axis in agreement with the above results (Fig. 5c). The gradient of *cyclin D1* expression across the DV axis is smoother than the expression of RFP from pTOPRed. We believe that the roughness of the RFP expression gradient is due to the variable levels of transfection achieved by electroporation, which is evident in the variable levels of GFP expression from pCIG (Fig. 5a). The gradient of Wnt signaling revealed by pTOPRed extends further ventrally than the gradient of Wnt signaling suggested by the expression of *cyclin D1*. This broader expression of pTOPRed across the DV axis may reflect the slow rate of degradation of RFP, which could cause its perdurance in ventral precursors as they are pushed away from the dorsal midline by proliferation. Cotransfection of pFOPRed, which has mutated TCF/Lef sites, with pCIG shows no RFP expression anywhere in the ventricular zone despite high levels of transfection revealed by GFP expression (Fig. 5d-f).

A dorsal-ventral gradient of growth in the spinal cord

Our evidence indicates that dorsal midline Wnts act as mitogens on neural precursors to increase their rate of

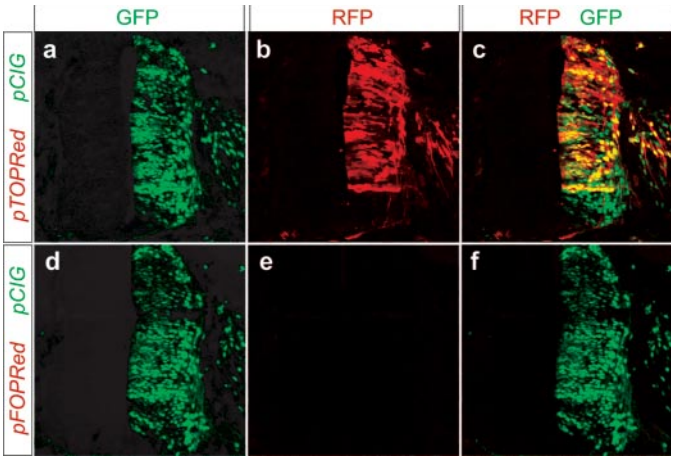

Fig. 5. An endogenous dorsal to ventral gradient of Wnt signaling. Cotransfection pTOPRed, a reporter construct containing synthetic TCF binding sites driving red fluorescent protein, with pCIG was used to investigate the range of β-catenin signaling in the neural tube. (a) GFP expression from pCIG shows the entire DV axis was transfected. (b) RFP from pTOPRed shows that the reporter is active across the dorsal three quarters of the neural tube and is more active in the dorsal-most quarter. The dorsal to ventral gradient of RFP expression is jagged, likely due to the variable levels of transfection between cells. By comparing the level of transfection of each cell as marked by GFP with the level of β-catenin signaling as marked by RFP, a gradient of β-catenin signaling across much of the DV axis is apparent in the merged image (c). (d-f) Transfection of pFOPRed in which the TCF binding sites are mutated shows no activity (e) despite high levels of cotransfection of pCIG (d). (f) Merged pFOPRed and pCIG images.

proliferation and decrease their rate of differentiation and that dorsal midline-derived Wnts are likely to form a dorsal to ventral activity gradient across the ventricular zone. These two observations imply that at intermediate stages of spinal cord development the neural tube should contain a corresponding dorsal to ventral 'growth gradient'; there should exist a gradient of proliferation rates that is high dorsally and low ventrally and an inverse gradient of differentiation rates that is high ventrally and low dorsally.

To address these parameters, we measured the rate of proliferation, the rate of differentation, and the level of Wnt signaling in neural precursors in five equally spaced bins across the DV axis of the developing chick spinal cord at five different stages of development. Representative examples of the embryos involved in the BrdU/N-tubulin analysis of proliferation rates and differentiation rates are shown in Fig. 6a-e. Even from these single time points of BrdU labeling (4 hours), one can observe the general trend that at early stages the proliferation rate is uniformly high and the differentiation rate is uniformly low (Fig. 6a,b), while at later stages the proliferation rate is higher dorsally and the differentiation rate is higher ventrally (Fig. 6d,e). We used similar data from 4 replicates at 6 BrdU-labeling times for 5 stages to determine the proliferation and differentiation rates in 5 equally spaced bins across the DV axis (Fig. 6f-i). Several interesting trends are apparent in these data. There is an inverse correlation between the rates of proliferation and differentiation across both the DV and time axes indicating the close, mechanistic link between G_1 to S cell cycle progression and G_1 to G_0 cell cycle exit. There is a spatial growth gradient across the DV axis that emerges by stage 21 with the rate of proliferation being highest dorsally and the rate of differentiation highest ventrally, an observation previously established by classic tritiated thymidine studies (Altman and Bayer, 1984). There is also a temporal growth gradient with the overall proliferation rate decreasing with time and the overall differentiation rate increasing with time. The spatial and temporal pattern of Wnt signaling directly correlates with the pattern of proliferation rates and inversely correlates with the pattern of differentiation rates as predicted by the mitogenic activity and distribution of Wnts expressed in the dorsal midline (Fig. 6i). These data support a model in which a mitogen gradient formed by Wnts expressed in the dorsal midline causes a growth gradient across the DV axis that patterns the growth of the neural tube over an extended period of development.

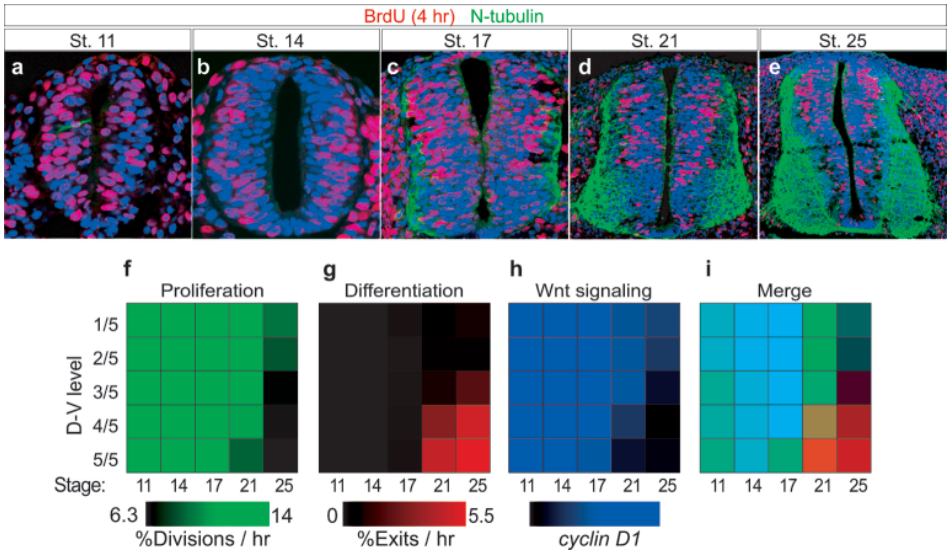

Fig. 6. An endogenous growth gradient in the spinal cord. The rates of proliferation and differentiation were determined by BrdU cumulative labeling (1, 2, 3, 4, 5 and 6 hours) and N-tubulin staining for 5 bins across the DV axis at HH stages 11, 14, 17, 21 and 25. (a-e) Representative images from each stage, labeled for 4 hours with BrdU and immunostained for BrdU and N-tubulin. A dorsal to ventral gradient of proliferation and a ventral to dorsal gradient of differentiation are apparent. The rates across space and time are represented by color intensity for (f) proliferation (green) and (g) differentiation (red). (h) The pattern of Wnt signaling determined by medial *cyclin D1* expression is shown in blue. (i) The proliferation rate, differentiation rate, and amount of Wnt signaling are merged to show the positive correlation between the proliferation rate and Wnt signaling and the inverse correlation between the differentiation rate and Wnt signaling. There is a growth gradient from early to late and dorsal to ventral that correlates with the pattern of Wnt signaling.

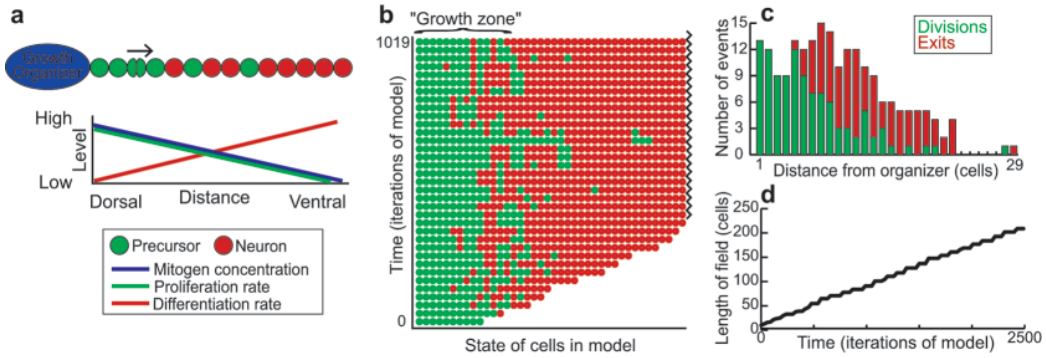

Fig. 7. Computer modeling demonstrates the mitogen gradient model can robustly pattern growth. (a) Diagram of the computer simulation of the mitogen gradient model. The proliferation rates and differentiation rates of a one-dimensional row of precursors are regulated by their distance from the growth organizer according to a linear function set by the user. Precursors are pushed ventrally away from the growth organizer when they divide. (b) To show the emergence of the growth zone, the state of cells in the model after every 30 iterations for the first 1020 iterations is shown. The squiggly line indicates where additional cells in the simulation are not shown. The growth zone is a robust and dynamically stable region whose size and shape is controlled by the proliferation and differentiation rate gradients and is independent of the starting number of precursors. (c) The mitogen gradient model can pattern cell cycle divisions and exits across a field of cells as seen in a chart of the total number of divisions and exits at each distance from the growth organizer after 1500 iterations of the simulation. The mitogen gradient model can also generate a constant rate of outgrowth and a constant supply of differentiated cells along an outgrowing structure. (d) The total length of the field of cells, including precursors and post-mitotic cells, at the end of every 30 iterations is shown. The total length of the field of cells increase roughly linearly with time.

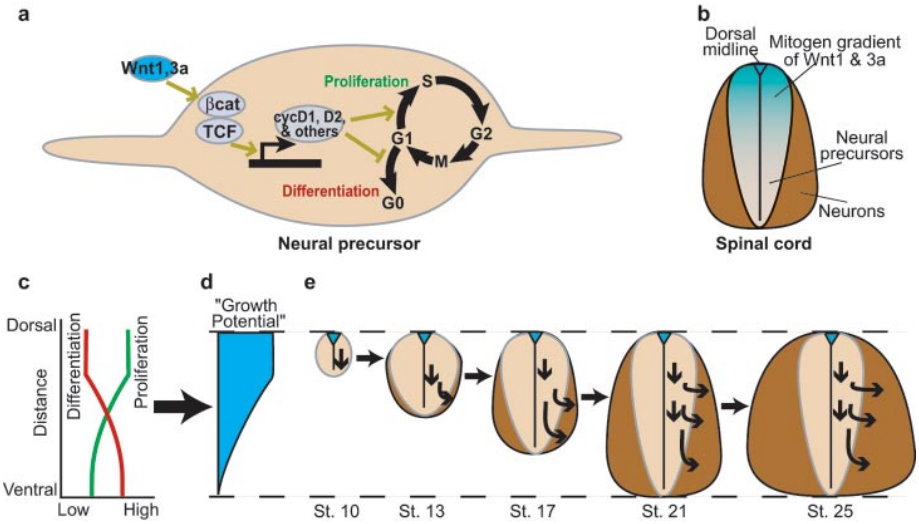

Fig. 8. Mitogen gradient model of how growth is patterned across the DV axis of spinal cord to determine its size and shape. (a) At the cellular level, Wnt1 and Wnt3a act as mitogens on neural precursors through the β-catenin pathway to promote cell cycle progression and inhibit cell cycle exit. (b) Diagram of cross section of the developing spinal cord. Mitotically active neural precursors comprise the medially located ventricular zone. Neural precursors exit the cell cycle and differentiate to form laterally located neurons. The mitogens Wnt1 and Wnt3a are expressed in the dorsal midline and form a dorsal to ventral concentration gradient across the field of neural precursors. (c) The potential size and shape of the mitogen gradient defines the potential rates of proliferation and differentiation across the DV axis. The proliferation and differentiation rate gradients level off dorsally because mitogenic Wnts are saturating at dorsal levels. The net effects of proliferation and differentiation form a gradient termed 'growth potential' (d). The proliferation rate gradient and the differentiation rate gradient cross about midway along the DV axis in this diagram. At this crossing point, the proliferation rate is equal to the differentiation rate meaning the population of precursors should be steady in number. Dorsal to this point the number of precursors is continually increasing, and ventral to this point the number of precursors is continually decreasing. The ventral extent of the growth potential gradient corresponds to the point at which the area between the curves above the crossing point equals the area between the curves below the crossing point such that the field of cells should not grow any further ventrally. (e) Different stages of the development of the spinal cord showing how it 'grows into' the size and shape specified by the growth potential gradient. The neural tube is initially small and round in cross section. At this early stage, Wnt1 and Wnt3a can diffuse across the entire DV axis to cause high rates of proliferation and low rates of differentiation across the entire DV axis. These high rates of proliferation and low rates of differentiation cause the neural tube to expand. As the neural tube expands, Wnt1 and Wnt3a become limiting at ventral levels causing higher rates of differentiation and lower rates of proliferation at ventral levels. This difference in growth potential across the DV axis causes the neural tube to become asymmetric; the ventricular zone becomes thicker dorsally than it is ventrally, and the mantle zone becomes thicker ventrally than it is dorsally. The neural tube continues to grow across its DV axis until it reaches a limit defined by the growth potential. Once this limit in DV size is reached, the developing spinal cord only grows across the medial-lateral and anterior-posterior axes by adding more neurons to the mantle zone. The arrows show the treadmilling movement of neural precursors ventrally away from the growth organizer caused by proliferation and the movement of precursors laterally to form neurons as they differentiate.

Computer simulation of the model

To explore the systems level dynamics of the mitogen gradient model, we developed a computer simulation of a generic, idealized mitogen gradient using a type of computer simulation termed agent-based modeling. Agent-based simulations consist of a collection of interacting autonomous units called agents that are programmed to respond to the environment or to other agents in defined ways. In our simulation, agents represent cells of two classes: mitotically active and post-mitotic. Agents representing mitotically active cells have two behaviors, proliferation and differentiation, whose rates are determined by the distance of the agent from the growth organizer. Post-mitotic cell agents have no behaviors; they can neither proliferate nor differentiate. When an agent representing a mitotically active cell proliferates, it results in two mitotically active cell agents and when it differentiates it results in one post-mitotic cell agent. The environment in our simulation consists of only a one-dimensional array of agents; that is, a single row of cells containing precursors and neurons. When an agent proliferates, the new agent pushes all the cells on the side opposite the growth organizer one cell diameter away from the growth organizer to make room for the new cell. This simulation does not attempt to model the diffusion of the mitogen from the growth organizer because that would needlessly complicate the model and the physical parameters of the diffusion of Wnts are unknown. Rather, this model simulates a generic, static mitogen gradient by allowing the user to graphically specify the rate of proliferation and the rate of differentiation as a linear function of distance from the growth organizer before the simulation is run. This computer model thus simulates a dynamic field of mitotically active cells and mitotically inactive cells in a static mitogen gradien (Fig. 7a). The simulation was implemented as a Java applet and can be used over the web at http://www.hombiosys.com/downloads/MitogenGradient.

We found that a growth zone, a dynamically stable region of mitotically active cells, emerges after several cell cycles. Proliferation in dorsal areas pushes precursors ventrally where they are more and more likely to differentiate (Fig. 7b). The growth zone thus represents an area of treadmilling of precursors ventrally. The growth zone is characterized by its size, which corresponds to how far from the growth organizer it extends, and its shape, which corresponds to the spatial pattern of differentiation. By varying the proliferation and differentiation rate gradients, we found that the size and shape of the growth zone are determined by the size and shape of the gradients of the proliferation and differentiation rates. Importantly, the size and shape of the growth zone once it reaches equilibrium is independent of the number of starting cells. This simplicity of control and emergent robustness are key attributes in systems biology and result because growth is under feedback control of size in the mitogen gradient model.

We also found that the mitogen gradient model can pattern the location of proliferation and differentiation (Fig. 7c). Most proliferation events happen dorsally and most differentiation events happen ventrally. The spatial pattern of differentiation is controlled primarily through the differentiation rate gradient. In the spinal cord, precursors move laterally out of the ventricular zone when they differentiate into neurons. The dorsal-ventral location of their exit from the cell cycle could play an important role in their eventual dorsal-ventral resting place.

Experimenting with the computer simulation of the mitogen gradient model showed that once the growth zone has reached dynamic equilibrium, it produces an outflow of differentiated cells at a fairly constant rate (Fig. 7d). The outflow rate of differentiated cells is dependent on both the proliferation and differentiation rate gradients. It is thus necessary to eventually shut off synthesis of the mitogen or the responsiveness of precursors to stop the flow of differentiated cells from the growth zone.

DISCUSSION

A mitogen gradient model for morphogenesis of the spinal cord

Our results support a mitogen gradient model for determining the size and shape of the developing spinal cord across the DV axis (Fig. 8). We have shown that Wnt1 and Wnt3a produced in the dorsal midline can act as mitogens on neural precursors by promoting their proliferation and inhibiting their differentiation through directly impinging on the cell cycle (Fig. 8a). We have produced several lines of evidence suggesting that mitogenic Wnts form a gradient across the ventricular zone as shown in the diagram (Fig. 8b). Firstly, the distribution of mitogenic Wnts, which seem to only be expressed in the dorsal midline, appears to be progressively subsaturating from dorsal to ventral across the neural tube based on the effects of ectopic expression of *Wnt1* and *Wnt3a*. Secondly, *cyclin D1*, a putatively direct transcriptional target of mitogenic Wnt signaling, is expressed in a dorsal to ventral gradient that extends approx. 20 cell diameters from the dorsal midline of the neural tube. And thirdly, a transcriptional reporter for mitogenic Wnt signaling is expressed at high levels dorsally and low levels ventrally. In this model, the mitogen gradient of Wnt1 and Wnt3a causes a gradient of proliferation potential across the DV axis that is high dorsally and a gradient of differentiation potential that is high ventrally (Fig. 8c). Our data demonstrate that there is a dorsal to ventral gradient of proliferation rates and ventral to dorsal gradient of differentiation rates that correlates with the expected gradient of mitogenic Wnts. We have also shown that mitogenic Wnts are saturating at dorsal levels and that the proliferation and differentiation rates correspondingly level off at dorsal levels. In our model, there is a net increase in neural precursors at dorsal levels because the proliferation rate is greater than the differentiation rate. At ventral levels where the differentiation rate is greater than the proliferation rate, there is a net decrease in precursor number. The ventral extent of the 'growth potential' is defined as the point at which these additive and subtractive effects balance out so that no precursors can treadmill past this point (Fig. 8d). The growth potential can extend much further ventrally than the mitogen gradient because it represents the cumulative effects of the proliferation rate being higher than the differentiation rate at dorsal levels. The ventral limit of the growth potential gradient thus defines the maximal size of the developing spinal cord across the DV axis and the developing spinal cord grows into the size and shape defined by the growth potential gradient (Fig. 8e).

With the present data, we are not able to directly compute the growth potential of the spinal cord because of the complexities of mitogen gradient formation and cell movement

and because of the limitations of the methods we used to calculate the proliferation rates and differentiation rates. Future experiments should quantify the mitogen gradient, the proliferation gradient, and the differentiation gradient with higher accuracy and resolution. These data would allow the morphogenesis of the spinal cord to be approached analytically and through computer simulation modeling.

Our data show that different Wnts have different mitogenic activities on spinal neural precursors in chick. These different activities and the mitogen gradient model of neural tube growth are supported by loss-of-function data from mice. In this model, one would expect *Wnt1/Wnt3a* double mutants to have smaller spinal cords. Disruption of *Wnt3a* causes truncation of the main body axis around the 7-somite level, making analysis of spinal cord growth difficult in *Wnt1/Wnt3a* double mutants. Despite this difficulty, *Wnt1/Wnt3a* double mutants do show a marked reduction in the number of neural precursors, with dorsal cell types being progressively more affected in the rostral spinal cord (Ikeya et al., 1997; S. M. Lee, M. Ishibashi, S. Takada and A. P. M., unpublished). *Wnt4* mutants and *Wnt7a*/*Wnt7b* double mutants have a neural tube that grows normally (B. Parr, M. Ishibashi and A. P. M., unpublished). The surprising result shown above that *Wnt3* is not mitogenic, cannot yet be supported through mutant analysis because *Wnt3* null mutants do not gastrulate (Liu et al., 1999). Furthermore, deletion of the dorsal midline and its resident Wnts through mutation of *Lmx1a* (Millonig et al., 2000) or targeted expression of diphtheria toxin (Lee et al., 2000a) causes a marked reduction in the size of the spinal cord.

Wnts are proposed to act as long-range signals (~100 μm) in the model presented here. However, the range of diffusion of Wnts in vertebrates has long been in question. It has previously been thought that vertebrate Wnts may only act as short-range signals owing to their high affinity for proteoglycans in the extracellular matrix (Burrus, 1994). It has been diffilcult to directly address the range of diffusion of Wnts in vertebrates because of the difficulty in generating high affinity antibodies. However, several lines of evidence have shown that the *Drosophila* Wnt family member Wingless, for which high affinity antibodies do exist, can act as a long-range signal in *Drosophila* (Zecca et al., 1996; Stringini and Cohen, 2000).

The mitogen gradient model results in continual growth of a field of cells, as shown by the computer simulation. An additional mechanism is thus necessary to terminate the lateral expansion of the neural tube once its proper size is achieved. How growth is ended in the neural tube is not clear but it may happen in part by a reduction in *Wnt1* and *Wnt3a* expression as neurogenesis nears completion (data not shown) and/or through a change in the competence of precursors to respond to Wnt signaling.

A considerable amount is known about the mechanisms regulating neural cell type specification in the spinal cord (Lee and Jessell, 1999; Briscoe et al., 2000; Jessell, 2000). A significant question therefore is: how are the mechanisms regulating growth and neural specification integrated? In the simplest model, these processes could be largely independent. A Wnt mitogen gradient could pattern the rates of proliferation and differentiation of neural precursors and opposing morphogen gradients of dorsally supplied TGFβs and ventrally supplied sonic hedgehog (Shh) could pattern the cell type identities of precursors. In practice, however, the processes of growth and neural specification are likely interlinked to ensure their appropriate timing. For example, the expression of transcription factors that regulate cell type is linked with the cell cycle status of the cell. Members of the Pax, Nkx, and Dbx families tend to be expressed in mitotically active neural precursors while members of Lmx family and MNR2 tend to be expressed in cells that will soon be or are already post-mitotic. It is likely that these transcription factors can modify the response of cells to the proposed Wnt mitogen gradient and vice versa. There are also other pathways including the Notch (Kageyama and Ohtsuka, 1999) and FGF (Tropepe et al., 1999) pathways that likely regulate growth in the neural tube. How all of these pathways are integrated with the proposed Wnt mitogen gradient model to generate the proper number and placement of each type of cell in the neural tube remains to be determined.

Mitogen gradient models in other processes

Julian Huxley first coined the terms ‘growth-gradient’ and ‘growth potential’ and developed theories of growth based on growth gradients in his classic treatise *Problems of Relative Growth* published in 1932. Huxley discovered growth gradients while studying the growth of appendages of male fiddler crabs. Male fiddler crabs contain one very large claw used in courtship that is held up like a fiddle. This claw is small in young males but is much larger relative to the rest of the body in older adults. This differential rate of growth of one part of the body relative to the rest of the body is called heterogony. By measuring the weight of each segment of the leg across populations of male fiddler crabs of different ages, Huxley discovered that each segment of the leg has a progressively higher degree of heterogony towards the fiddle-like claw. The chela (claw) grows the most quickly and more proximal segments grow progressively more slowly. Huxley termed this progressive change in heterogony across space a ‘growth gradient’ and went on to show that growth gradients exist in many other animals. Huxley termed the high point of the growth gradient, such as the chela, the ‘growth center’. Our biochemical understanding of development was very poor at this time, but Huxley extrapolated from other gradient models of his contemporaries to postulate the existence of an “initial chemodifferentiative localization of high growth-potential in the male chela” (p. 169). The essence of this model is thus similar to the mitogen gradient model, but since the molecular understanding of biology was very poor at that time, he could not describe the mechanisms and implications of growth gradients. In the present model, we use the term growth organizer instead of growth-center to emphasize the similarities of this model with the widely known morphogen gradient model. Unlike Huxley’s growth-center, the growth organizer does not necessarily grow itself. The roof plate, a source of mitogenic Wnts, has a low proliferation rate. Preventing the growth organizer from growing may ensure a steady and fixed supply of mitogen.

In developing and experimenting with the computer simulation of the mitogen gradient model, two corollaries to the model became apparent. The first is that the CNS adds a process of orthogonal differentiation to the mitogen gradient model. When neural precursors differentiate to form neurons, they migrate laterally out of the ventricular zone and thus out of the treadmilling field of precursors. This movement

orthogonal to the mitogen gradient limits the dorsal-ventral growth of the neural tube so it does not form a long chain of differentiated cells as happens in the computer simulation. Orthogonal differentiation can also pattern the placement of differentiated cells. Other systems that might employ a mitogen gradient mechanism such as the tailbud or limb bud do not seem to utilize orthogonal differentiation. The second corollary uses a mitogen gradient to control the rate of outgrowth. The model shows that once the growth zone reaches dynamic equilibrium, differentiated cells flow from the growth zone at a constant rate. The mitogen gradient model can thus simply and robustly control the rate of outgrowth and timing of differentiation. Such a mechanism could be at work in diverse developmental processes, such as growth of the endochondral skeleton, tailbud, and limb bud, where differentiated cells are continually laid down behind an outwardly moving growth zone.

Mitogen gradients and morphogen gradients

The mitogen gradient model proposed here combines aspects of Huxley's ideas and the now widely accepted morphogen gradient model, which is used to explain the cell-fate patterning effects of the amphibian organizer and other patterning centers. In both the morphogen and mitogen gradient models, a diffusible molecule produced in an organizer forms a concentration gradient across a field of cells. In the morphogen gradient model, the local concentration of the diffusible molecule specifies cell fate at different thresholds of concentration. In the mitogen gradient model, the local concentration of the diffusible molecule determines cells' rates of proliferation and differentiation as a continuous function of concentration without using thresholds. Another difference is that in the mitogen gradient model, the movement of cells through the concentration gradient as the field of cells expands is of central importance. The morphogen gradient model can be envisioned to occur in a field of cells of static size with cells not moving relative to the organizer. The morphogen and mitogen gradient models are thus similar in their use of organizers that generate concentration gradients but differ in the targets of the signaling molecules, their use of thresholds, and in the importance of cell movement through the gradient.

From egg to embryo there is a large increase in the both the number of cell types and the total number of cells. The patterning of cell types and the patterning of cell numbers occur concurrently in many developmental processes and the mechanisms that regulate these processes are thus likely coordinated. One possibility is that growth and form are coordinated during morphogenesis through the interaction of mitogen and morphogen gradients. In the developing spinal cord for example, sonic hedgehog acts as a ventral morphogen produced by the floor plate to pattern the ventral neural tube. One target of Shh is the transcription factor Pax6, which it represses as a function of concentration (Briscoe et al., 2000). Pax6 is involved in the regulation of transcription factors that specify cell fate such as the motor neuron determinant MNR2 (Tanabe et al., 1998). Pax6 is also required for the activation the Wnt antagonist Sfrp2 (Kim et al., 2001). Both Pax6 and Sfrp2 are expressed in neural precursors that form motor neurons. Taken together, these data suggest a model in which the Shh morphogen gradient could shape the Wnt mitogen gradient through indirect repression of a Wnt antagonist in the ventral neural tube to regulate the timing and placement of motor neuron differentiation. In other processes such as morphogenesis of the fly wing, morphogen and mitogen gradient mechanisms could be combined using the same signaling molecules that act as both morphogens and mitogens.

Conclusions

The mitogen gradient model has several appealing features at the systems level. Firstly, a simple mechanism can regulate a dynamic process. The size and shape of a tissue can be determined simply by the size and shape of a mitogen gradient. Secondly, this model is inherently robust because the growth of a tissue is under feedback control by its size. Lastly, the mitogen gradient model is highly evolvable. A mitogen gradient can evolve from a morphogen gradient by the acquisition of new targets that regulate the cell cycle. Differences between species may often be driven more by changes in cell numbers rather than changes in cell types. Evolutionary changes in the shape and size of tissues could be achieved by simply altering the shape and size of the mitogen gradient. We feel the mitogen gradient model could be a widely used mechanism for determining tissue size in plants and animals.

We thank Charles Sherr, Osamu Tetsu, Hans Clevers, Vincent Kidd, and Makoto Ishibashi for reagents, Doug Melton, Catherine Dulac, Connie Cepko, and members of the McMahon lab for useful input, and Mark Wijgerde, Shigemi Hayashi, and Makoto Ishibashi for comments on the manuscript. S. G. M. is supported by a predoctoral fellowship from HHMI. Work in A. P. M.'s laboratory was supported by a grant from the NIH (HD 30249).

REFERENCES

Altman, J. and Bayer, S. A. (1984). *The Development of the Rat Spinal Cord*. New York: Springer-Verlag.

Briscoe, J., Pierani, A., Jessell, T. M. and Ericson, J. (2000). A homeodomain protein code specifies progenitor cell identity and neuronal fate in the ventral neural tube. *Cell* **101**, 435-445.

Burrus, L. (1994). Wnt-1 as a short range signaling molecule. *BioEssays* **16**, 155-157.

Cho, E. A. and Dressler G. R. (1998). TCF-4 binds beta-catenin and is expressed in distinct regions of the embryonic brain and limbs. *Mech. Dev.* **77**, 9-18.

Conlon, I. and Raff, M. (1999). Size control in animal development. *Cell* **96**, 235-244.

Day, S. J. and Lawrence, P. A. (2000). Measuring dimensions: the regulation of size and shape. *Development* **127**, 2977-2987.

Dickinson, M. E., Krumlauf, R. and McMahon, A. P. (1994). Evidence for a mitogenic effect of Wnt-1 in the developing mammalian central nervous system. *Development* **120**, 1453-1471.

Diehl, J. A. and Sherr, C. J. (1997). A dominant-negative cyclin D1 mutant prevents nuclear import of cyclin-dependent kinase 4 (CDK4) and its phosphorylation by CDK-activating kinase. *Mol. Cell. Biol.* **17**, 7362-7374.

Fantl, V., Stamp, G., Andrews, A., Rosewell, I. and Dickson, C. (1995). Mice lacking cyclin D1 are small and show defects in eye and mammary gland development. *Genes Dev.* **9**, 2364-2372.

Gavin, B., McMahon, J. and McMahon, A. P. (1990). Expression of multiple novel *int-1/wnt-1*-related genes suggests a major role for the *wnt-1* family of putative signaling molecules during fetal mouse development. *Genes Dev.* **4**, 2319-2332.

Hollyday, M., McMahon, J. A. and McMahon, A. P. (1995). Wnt expression patterns in the chick embryo nervous system. *Mech. Dev.* **52**, 9-25.

Huxley, J. S. (1932). *Problems of Relative Growth.* London: Butler and Tanner Ltd.

Ikeya, M., Lee, S. M. K., Johnson, J. E., McMahon, A. P. and Takada, S. (1997). Wnt signaling required for expansion of neural crest and CNS progenitors. *Nature* **389**, 966-970.

Jessell, T. M. (2000). Neuronal specification in the spinal cord: inductive signals and transcriptional codes. *Nat. Rev. Genet.* **1**, 20-29.

Kageyama, R. and Ohtsuka, T. (1999) The Notch-Hes pathway in mammalian neural development. *Cell Res.* **9**, 179-188.

Kim, A. S., Anderson, S. A., Rubenstein, J. L., Lowenstein, D. H. and Pleasure, S. J. (2001). Pax-6 regulates expression of SFRP-2 and Wnt-7b in the developing CNS. *J. Neurosci,* **21**, RC132 1-5.

Korinek, V., Barker, N., Willert, K., Molenaar, M., Roose, J., Wagenaar, G., Markman, M., Lamers, W., Destree, O. and Clevers, M. (1997). Constitutive transcriptional activation by a β-catenin-TCF complex in $APC^{-/-}$ colon carcinoma. *Science* **275**, 1784-1787.

Korinek, V., Barker, N., Morin, P. J., van Wicken, D., de Weger, R., Kinzler, K. W., Vogelstein, B. and Clevers, M. (1998). Two members of the Tcf family implicated in Wnt/β-catenin signaling during embryogenesis in the mouse. *Mol. Cell. Biol.* **18**, 1248-1256.

Kuhl, M., Sheldahl, L. C., Park, M., Miller, J. R. and Moon, R. T. (2000). The Wnt/Ca^{2+} pathway: a new vertebrate Wnt signaling pathway takes shape. *Trends Genet.* **16**, 279-283.

Lahti, J. M., Li, H. and Kidd, V. J. (1997). Elimination of cyclin D1 in vertebrate cells leads to an altered cell cycle phenotype, which is rescued by overexpression of murine cyclins D1, D2, or D3 but not by a mutant cyclin D1. *J. Biol. Chem.* **272**, 10859-10869.

Lee, K. J. and Jessell, T. M. (1999). The specification of dorsal cell fates in the vertebrate central nervous system. *Annu. Rev. Neurosci.* **22**, 261-294.

Lee, K. J., Dietrich, P. and Jessell, T. M. (2000a). Genetic ablation reveals that the roof plate is essential for dorsal interneuron specification. *Nature* **403**, 734-740.

Lee, S. M., Tole, S., Grove, E. and McMahon, A. P. (2000b). A local Wnt-3a signal is required for development of the mammalian hippocampus. *Development* **127**, 457-467.

Li, H., Grenet, J. and Kidd, V. J. (1995). Structure and gene expression of avian cyclin D2. *Gene* **167**, 341-342.

Liu, P., Wakamiya, M., Shea, M. J., Albrecht, U., Behringer, R. R. and Bradley, A. (1999) Requirement for Wnt3 in vertebrate axis formation. *Nat. Genet.* **22**, 361-365.

Matsushime, H., Roussel, M. F., Ashmun, R. A. and Sherr, C. J. (1991). Colony stimulating factor 1 regulates novel cyclins during the G1 phase of the cell cycle. *Cell* **17**, 701-713.

McMahon, A. P. and Bradley, A. (1990). The *wnt-1* (*int-1*) proto-oncogene is required for development of a large region of the mouse brain. *Cell* **62**, 1073-1085.

Millonig, J. H., Millen, K. J. and Hatten, M. E. (2000). The mouse *dreher* gene (*Lmx1a*) controls formation of the roof plate in the vertebrate CNS. *Nature* **403**, 764-769.

Nakamura, H., Watanabe, Y. and Funahashi, J. (2000). Misexpression of genes in brain vesicles by *in ovo* electroporation. *Dev. Growth Differ.* **42**, 199-201.

Niwa, H., Yamamura, K. and Miyazaki, J. (1991). Efficient selection for high-expression transfectants with a novel eukaryotic vector. *Gene* **15**, 193-199.

Nurse, P. (2000). A long twentieth century of the cell cycle and beyond. *Cell* **100**, 71-78.

Nusse, R. (2001). The Wnt gene homepage. *http://www-leland.stanford.edu/~rnusse/wntwindow.html*

Parr, B. A., Shea, M. J., Vassileva, G. and McMahon, A. P. (1993). Mouse *Wnt* genes exhibit discrete domains of expression in the early embryonic CNS and limb buds. *Development* **119**, 247-261.

Roelink, H., Wagenaar, E., Lopes da Silva, S. and Nusse, R. (1990). Wnt-3, a gene activated by proviral insertion in mouse mammary tumors, is homologous to int-1/Wnt-1 and is normally expressed in mouse embryos and adult brain. *Proc. Natl. Acad. Sci. USA* **87**, 4519-4523.

Shtutman, M., Zhurinsky, J., Simcha, I., Albanese, C., D'Amico, M., Pestell, R. and Ben-Ze'ev, A. (1999). The cyclin D1 gene is a target of the β-catenin/LEF-1 pathway. *Proc. Natl. Acad. Sci. USA* **96**, 5522-5527.

Sicinski, P., Donaher, J. L., Parker, S. B., Li, T., Fazeli, A., Gardner, H., Haslam, S. Z., Bronson, R. T., Elledge, S. J. and Weinberg, R. A. (1995). Cyclin D1 provides a link between development and oncogenesis in the retina and breast. *Cell* **82**, 621-630.

Stringini, M. and Cohen, S. M. (2000). Wingless gradient formation in the Drosophila wing. *Curr. Biol.* **10**, 293-300.

Tanabe, Y. and Jessell, T. M. (1996). Diversity and pattern in the developing spinal cord. *Science* **274**, 1115-1123.

Tanabe, Y., William, C. and Jessell, T. M. (1998). Specification of motor neuron identity by the MNR2 homeodomain protein. *Cell* **95**, 67-80.

Tetsu, O. and McCormick, F. (1999). β-Catenin regulates expression of cyclin D1 in colon carcinoma cells. *Nature* **398**, 422-426.

Thomas, K. R. and Capecchi, M. R. (1990). Targeted disruption of the murine int-1 proto-oncogene resulting in severe abnormalities in midbrain and cerebellar development. *Nature* **346**, 847-850.

Tropepe, V., Sibilia, M., Ciruna, B. G., Rossant, J., Wagner, E. F. and van der Kooy, D. (1999) Distinct neural stem cells proliferate in response to EGF and FGF in the developing mouse telencephalon. *Dev Biol.* **208**, 166-188.

Zecca, M., Basler, K. and Struhl, G. (1996). Direct and long-range action of a wingless morphogen gradient. *Cell* **87**, 833-844.